Progress In Electromagnetics Research, Vol. 118, 397–414, 2011

A QUASI THREE-DIMENSIONAL RAY TRACING METHOD BASED ON THE VIRTUAL SOURCE TREE IN URBAN MICROCELLULAR ENVIRONMENTS

Z.-Y. Liu* **and L.-X. Guo**

School of Science, Xidian University, No. 2, Taibai Road, Xi'an, Shaanxi, China

Abstract—The increase in mobile communications traffic has led to heightened interest in the use of ray tracing (RT) methods together with digital building databases for obtaining more accurate and efficient propagation prediction in urban microcellular environments. In this paper, a novel quasi three-dimensional (3-D) RT algorithm is presented by taking into account the advantages of both the image theory (IT) and the shooting-and- bouncing ray (SBR) method. It is based on creating a new virtual source tree in which the relationship between neighbor nodes is a left-son-and-right-brother one. Our theoretical results of the signal path loss along the streets are compared with measurements which have been reported for city streets in Tokyo and Ottawa City for various values of the propagation parameters. The good agreement with these measurements indicates that our prediction model works well for such microcellular communication applications. The proposed method can provide the reliable theory basis for radio-wave propagation prediction and network planning in urban microcellular environments.

1. INTRODUCTION

During the last decade, the progressive deployment of the first extensive public mobile radio networks has spurred researchers toward the study of radio propagation in urban environment and the development of fast and reliable radio coverage prediction models [1, 2]. At present, the propagation prediction model can be mainly divided into two categories: one is statistical model, and the other is deterministic model. Several statistical [3–5] and

Received 16 April 2011, Accepted 30 June 2011, Scheduled 7 July 2011

* Corresponding author: Zhong-Yu Liu (liuzhongyu2003@163.com).

deterministic models [6–12] have been reported in the literature for the estimation of a variety of signal-propagation characteristics in urban environment. The most widely used statistical models are based on closed mathematical formulas, obtained using statistical analysis of measurements taken in the area of interest. These models are simple to use but do not give site-specific prediction, requiring supplementary on-site measurement data [13]. To overcome those problems, the deterministic propagation models, which are principally based on numerical methods such as the ray tracing (RT) method and the finite-difference time-domain (FDTD) method [14], are developed and widely adopted. Of those, the RT method combined with uniform theory of diffraction (UTD) [15] is most frequently applied to radio coverage prediction [16–19]. This method is used to identify all possible ray paths between a transmitter (Tx) and a receiver (Rx) in multipath channels. Once all possible paths have been identified, high-frequency electromagnetic techniques, such as UTD, are applied to the rays to compute the amplitude, phase, delay, and polarization of each ray [20]. The RT models potentially represent the most accurate and versatile methods for urban and indoor, multipath propagation characterization or prediction. Generally, such models are used in the planning phase of mobile radio networks, where their accuracy may in principle lead to great advantages in terms of deployment cost reduction and service quality increase [21].

Nevertheless, the widespread adoption of RT methods is still limited due to the high complexity and high computation time of the corresponding computer programs [21–23]. And, for the conventional RT algorithms such as ray tube method [17], the prediction accuracy is not satisfactory. Such algorithms are generally based on shooting-and-bouncing ray (SBR) or image theory (IT) techniques [24]. According to the SBR method, rays are launched with a specific angular separation from source points, so that no building faces are missed at large distances from the Rx, and their paths are traced until a certain power threshold is reached [25]. The IT takes into consideration all walls and obstacles as potential reflectors and evaluates the location of their base station images. This imaging technique works by conceptually generating an image tree for each base station location. This image information is then stored and used for computing the channel characteristics at each user location. The IT technique can guarantee high accuracy, but suffers from inefficiency when the number of walls involved is large and reflection times are high [26].

In this paper, in order to overcome the drawbacks of SBR method and IT and retain their merits, a RT method for the calculation of radio coverage in urban microcellular environment using the new virtual

source tree, which is based on the numerical simulation of geometrical optics (GO) and UTD and can solve some of the problems that other RT methods have, is presented. Comparing with the conventional ray tube method [17], the results of the proposed method in this paper show better agreement with the measurements.

2. THEORY OF NEW VIRTUAL SOURCE TREE

2.1. Three Types of Sources

To illustrate the theory of new virtual source tree, three types of sources must be defined (see Fig. 1); the transmitter, reflection, and diffraction sources on the plan view of the quasi three- dimensional (3-D) environment and they are generated from site-specific information.

The transmitter source represents transmitting antenna and is described by the position of the Tx and the visibility angle of 2π radian. This source is the starting point of all propagation paths arriving at Rx. Due to the existence of surrounding walls and corners, the reflected and diffracted rays, which are respectively defined as reflection and diffraction rays, are generated by the rays from transmitter source.

The reflection source is actually a virtual source and represents the image with respect to the wall. It is described by the position of the image on the wall and the visibility angle less than π. Its image is one of the multiple reflected images of a Tx or building corners as secondary source. The visibility angle of reflection source is determined by the illuminated portion of the wall and represented by two unit vectors $\hat{\mathbf{n}}_{r1}$ and $\hat{\mathbf{n}}_{r2}$, as shown in Fig. 1. Basically, it has a fan-like shape but its

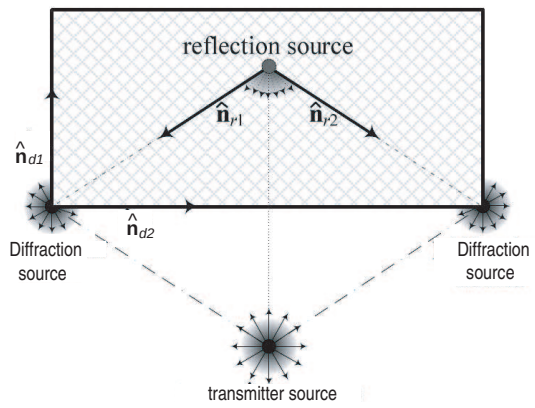

Figure 1. Three types of sources and corresponding "visibility angle".

valid region is confined by the corresponding wall and the blockage of walls and corners in its interior region. The reflection sources can be generated by all kinds of precedent sources when they illuminate the wall in their valid region.

The diffraction source is generated as a child of three types of precedent sources. It is described by the position of the corner, the corner number, and the visibility angle. The visibility angle is determined by two walls adjacent to the corner and described by two unit vectors $\hat{\mathbf{n}}_{d1}$ and $\hat{\mathbf{n}}_{d2}$, as shown in Fig. 1. And the most common values of the visibility angle are $\pi/2$ and $3\pi/2$ for buildings in urban environment. It also has a fan-like shape, and the children of the diffraction source are generated from the blockage of the scatters in its valid region.

2.2. Construction of a Virtual Source Tree

In order to store as much information as possible by taking up as little space as possible in the computer's memory, a new storage structure is designed and depicted in Fig. 2. Each node in this tree stores essential information. Thus, large amounts of memory can be saved when the depth of the tree is big. The root of the virtual source tree is the transmitter source and the lower order virtual sources of this tree are the precondition for generating the higher order virtual sources. Starting with any node toward its left child in the virtual

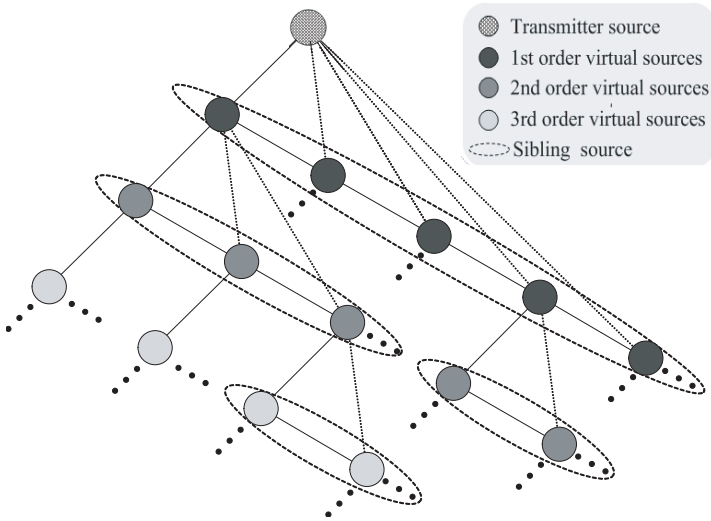

Figure 2. The construction of new virtual source tree.

source tree, the order of the node would be increased by one for passing through each node. Starting with any node toward its right child in the virtual source tree, if we traverse the nodes by following each pointer to the next node until no right child can be found, a single-linked list composed by these nodes would be achieved. In this single-linked list, all the nodes have a common order and are generated by the same source. So, these nodes are vividly defined as sibling source. Fig. 2 presents four different sibling sources which are marked by the dotted ellipse. Based on the virtual source tree as illustrated in Fig. 2, it can be seen that the relationship between each node and its left child is analogous to the relationship between a father and a son, whereas, the relationship between each node and its right child is similar to the relation between siblings. All the nodes in the tree are stored in the form of the binary tree, i.e., the topology construction is composed of different circles and thick solid lines in Fig. 2. In order to determine the propagation paths from a Tx to a Rx with higher efficiency, each virtual source in the same sibling source has a pointer to the common father node and this pointer is visually presented by dotted lines in

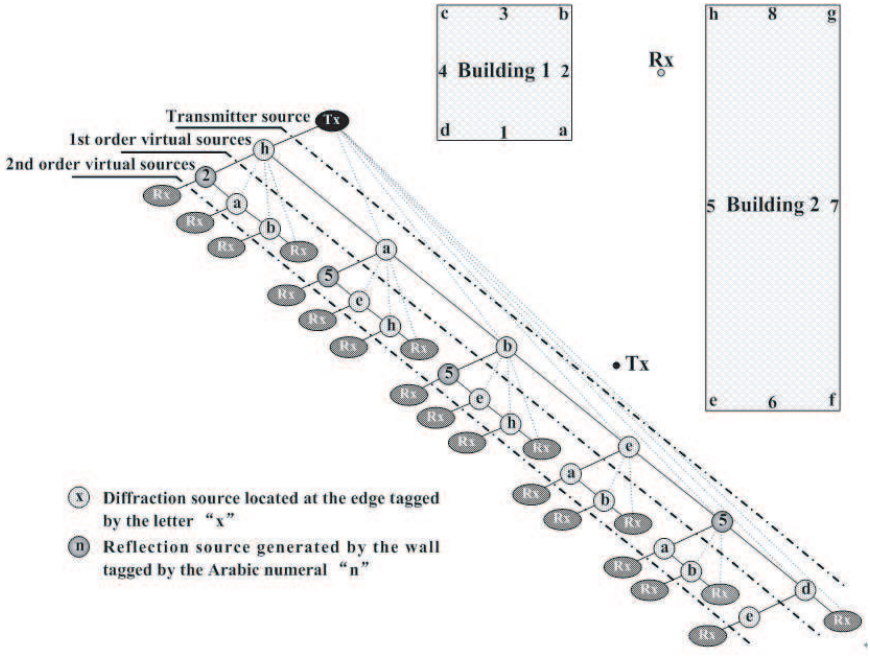

Figure 3. Example of 2-D building layout and corresponding virtual source tree. Walls are tagged by Arabic numerals and edges by letters.

Fig. 2. According to the above analysis, the construction of the new virtual source tree, which is proposed in this paper, looks very much like a binary tree. And the relation between the neighbor nodes in the tree is a left-son-and-right-brother one.

In Fig. 3, an example of the constructing a virtual source tree (excepting the Rx in the structure of the binary tree) for the plan view of a simplified environment made of two rectangular buildings is presented. The maximum order of the virtual source tree is two. Each building has four walls and four corners. The walls are numbered from "1 to 8" and the corners are labeled with the alphabet from "a to h".

2.3. Procedure for Creating Virtual Source Tree

In the process of constructing the virtual source tree, two terms must be defined, i.e., the type weight of the ray and limit number. When radio-wave transmitting under urban microcell, diffraction loss is so much more than reflection loss generally that it is quite necessary to distinguish reflection and diffraction using the type weight of the ray. Therefore, the new concept of type weight is introduced. When doing some simulation in this paper, the type weight of reflection and diffraction are fixed to be 1 and 3, respectively. Meanwhile, the limit number, which determines the depth of virtual source tree, is equal to an allowable maximum of the sum of type weight for each propagation path.

Figure 4 presents a simplified flow diagram of constructing a virtual source tree. If we follow this flow diagram, a virtual source tree can be built as shown in Fig. 2. The main steps of constructing the virtual source tree are the following:

(1) All the visible walls and corners of the transmitter source should be found out firstly. In the process of determining the visible walls of the transmitter source, the part of the wall, which is blocked by the other walls, needs to be discarded, and this can avoid checking if the propagation paths from Tx to Rx actually exist. All the reflection sources, which are images of the transmitter source with respect to visible walls, and diffraction sources, which are described by the position of visible corners of the transmitter source, constitute the first order virtual sources.
(2) After determining the first order virtual sources (i.e., the sibling source generated by the common transmitter source), for all the reflection sources and diffraction sources, the same operations are carried out as step (1), taking into account the search area restrictions for each propagation mechanism considered. All the virtual sources of the second order virtual sources are determined

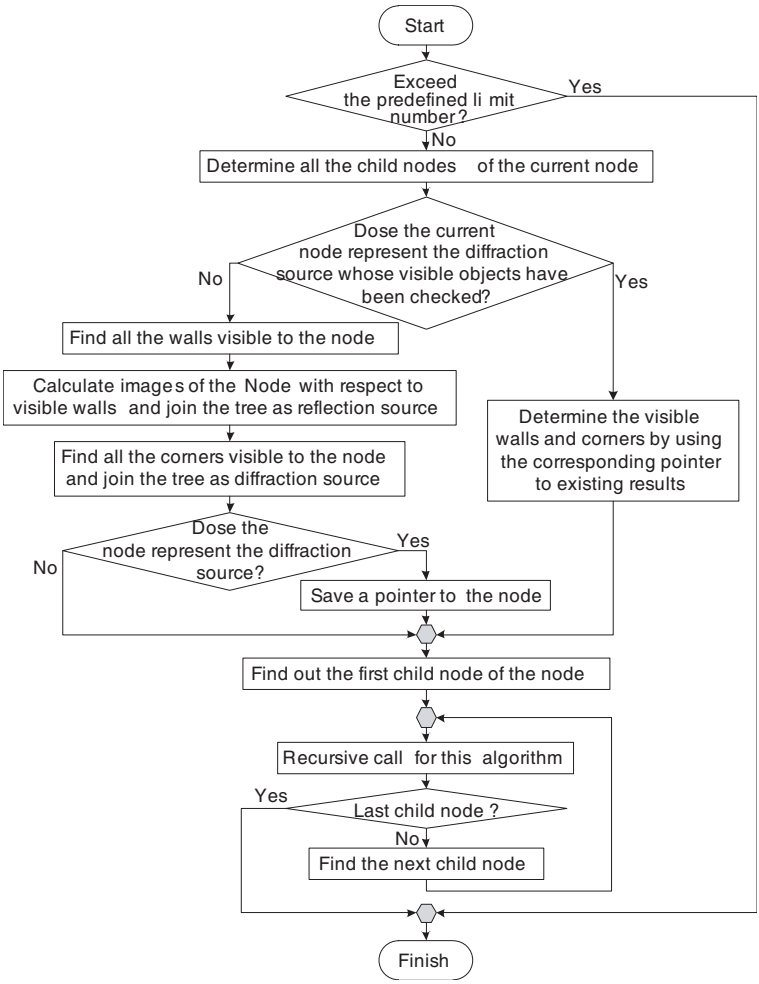

Figure 4. Simplified flow diagram of constructing a virtual source tree.

by the above operation. What calls for special attention is that all the visible walls and corners for each diffraction sources need to be kept in one contiguous memory and saved pointers to this storage space. This way of dealing with the diffraction source can avoid repeated calculation.

(3) For all the reflection sources in the second order virtual sources, the same operations are carried out as step (2) for the reflection source. But before execution of finding the visible walls and corners for each diffraction source, one has to check if the

diffraction source belongs to the lower order virtual sources. If yes, instead of finding out the visible objects based on intersection test of a ray with an object, the visible walls and corners will be determined only by using the corresponding pointer to existing results; otherwise, the same operations are performed as step (2) for the diffraction source. All the virtual sources determined in this step make up the third order virtual sources.

(4) By repeating above recursive process, the higher order of the virtual sources will be got and the virtual source tree will be completed until the predefined limit number is exceeded.

3. RAY TRACING METHOD BASED ON NEW TREE STRUCTURE

The proposed method in this paper is developed for a quasi 3-D environment, i.e., building walls are assumed to be much higher than both the Tx and Rx height so that diffractions and reflections from the rooftops are neglected. The ground is assumed flat, such that all vertical obstacle edges are perpendicular to ground and, consequently, parallel to each other. All the propagation paths with possible combinations of wall reflections and corner diffractions can be found by the virtual source tree. Once the trajectories from Tx to Rx are determined, the signal path loss would be obtained.

In the process of executing RT algorithm in this paper, the generation of the virtual source tree, the determination of propagation paths and the field calculations are performed simultaneously and are finished at the same time. Thus, the time of virtual source tree traversal can be avoided and the storage space which stores a large amount of propagation paths can be saved. The proposed RT method is described by the flow chart shown in Fig. 5 and contains four fundamental steps:

Step 1) Loading microcellular environment database: the building layouts built with different digital map, wall material characteristics, dimensions and locations of buildings, and positions of Txs and Rxs.

Step 2) Creation of the virtual source tree: the different order of the virtual source with respect to the building walls and building corners are determined, according to the procedure described in Section 2.3.

Step 3) Finding propagation paths: Once the virtual source tree is completed, ray-tracing routine is employed to find all the two-dimensional (2-D) propagation paths. Since the construction of the virtual source tree is independent of the location of Rx, the tree can be used for any Rx location without reconstructing it. In order to

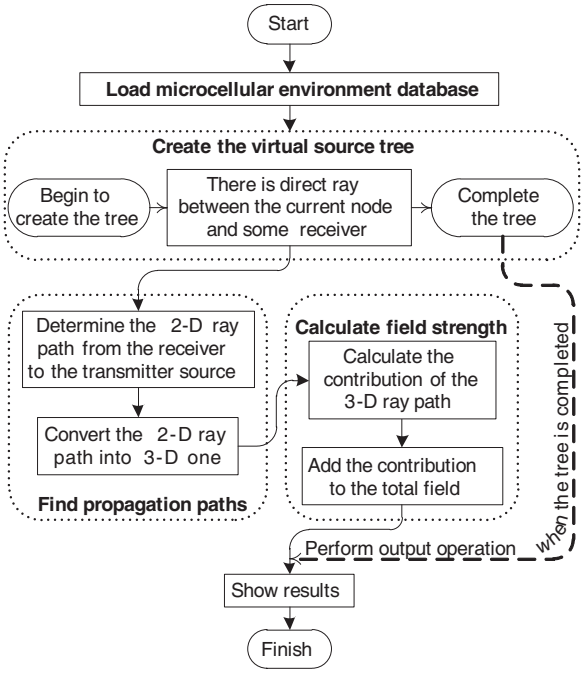

Figure 5. Flowchart of proposed RT method.

show the process of finding propagation paths, we take the same case as shown in Fig. 3 for example. For a given location of a Rx, one should first check if some source, which belongs to the virtual source tree (the structure of the tree excepting the Rx in Fig. 3), is visible to the Rx (for line-of-sight rays). If yes, the Rx is added to the sibling source generated by this source. After checking all of the sources in the tree, the virtual source tree (including Rx) can be completed as shown in Fig. 3. Then, all 2-D propagation paths will be got by tracing from each Rx to the transmitter source. These ray paths are depicted in Fig. 6. All the 2-D propagation rays are converted into their 3-D counterparts following the procedure detailed in [24]. The conversion of 2-D ray path into 3-D trajectories is performed with the help of the total distance measured along the 2-D path and the antennas heights with respect to the ground.

Step 4) Electromagnetic calculation: After all the trajectories between Tx and Rx have been individuated, the total field at each measurement point is computed by adding the contributions of all pertaining propagation paths. Each contribution due to a specific path is obtained by the following analysis and calculation.

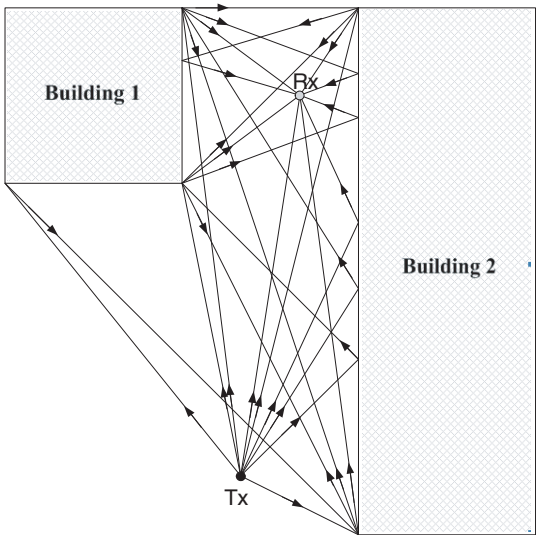

Figure 6. 2-D description of the propagation paths that can be followed to go from the Tx to the Rx corresponding virtual source tree in Fig. 3.

If a direct visibility path is considered, then the field strength depends only on the distance between the source and the observation point, and this field contribution is given by

$$\mathbf{E}_{LOS} = \mathbf{E}_0 \frac{e^{-jkr_0}}{r_0} \tag{1}$$

where k is the free-space wave number, and $\mathbf{E}_0$ is the electric field where located at 1 m from the source. The value r_0 represents the length of the directed path.

If reflections or diffractions are involved, the field strength is calculated by Eq. (2), i.e.,

$$\mathbf{E} = \frac{\mathbf{E}_0}{r_1} \cdot \prod_{i=1}^{n} (\mathbf{R}_i A r_i) \cdot \prod_{i=1}^{m} (\mathbf{D}_i A d_i) \cdot e^{-jkr} \tag{2}$$

where the distance r_1 is the distance from Tx to the first reflection point or diffraction point, and r is the distance between the transmitter and the observation point. Ar_i and Ad_i are the spreading factor for a reflection from a surface, and for a diffraction at an edge, respectively. The values n and m represent the total number of reflection and diffraction. The dyadic quantities $\mathbf{R}_i$ and $\mathbf{D}_i$ correspond to reflection

coefficient and diffraction coefficient, respectively. More details of the calculation of the two coefficients can be traced in [27].

Once the trajectories are determined, the contribution of each propagation path to the total received electric field E_{total} can be obtained by Eq. (2). Thus, the path loss is calculated in dB as follows:

$$L = 20 \lg \left[\frac{\lambda}{4\pi} \left| \frac{E_{total}}{E_0} \right| \right] \tag{3}$$

where λ is the wavelength.

4. COMPARISON WITH PROPOSED METHOD AND MEASUREMENTS

In order to demonstrate the accuracy of the RT method proposed in Section 3, comparisons with published results in two high-rise urban environments are presented. In the first test scenario, it represents the core of Ottawa, Canada, for which measurements [28] for the vertical polarization at 910 MHz are available in the literature. This scene 900 m × 600 m area and consists of 130 obstacles (i.e., 130 buildings), comprising 614 faces and edges, as illustrated in Fig. 7. The base-station antenna (Tx) was mounted at 8.5 m above the ground, well below the rooftops, and the Rx, 3.65 m above the ground, was assumed to move along two parallel streets (Slater street and Queen street). The values of relative permittivity ε_r and conductivity σ are very important to the prediction results. Real building surfaces are made up of a

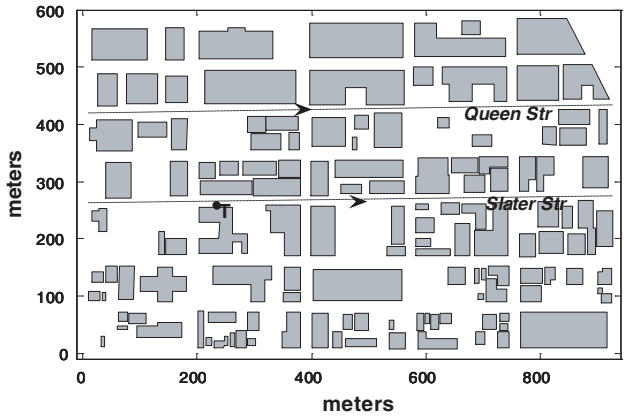

Figure 7. Plan view of the Ottawa city core. The Tx is at T, and Rxs placed along Slater St. and Queen St. (dotted line).

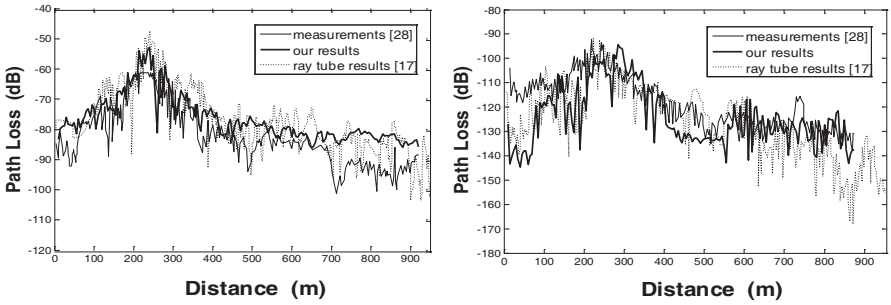

Figure 8. A comparison of the calculated and measured path loss characteristics for the mobile station moving along two parallel streets. (a) Along Slater Street. (b) Along Queen Street.

complex pattern of windows and other structures with different wall materials. The only practical method is to assign reasonable average values of ε_r and σ to characterize them [29]. In our calculations, the value of ε_r and σ was chosen as 9, 0.1 S/m for buildings and 15, 7 S/m for the ground. And the limit number is limited to seven.

Figure 8 shows the differences for the path-loss characteristics between the simulated predictions (thick solid line), ray tube results (dashed curve) [17], and the measurements (thin line) [28]. It could be observed that the present simulation model performed consistently well compared with the measurements. Figs. 8(a) and (b) present the path loss along Slater and Queen Streets, respectively. The former is a line-of-sight (LOS) street and the latter is an out-of-sight (OOS) street. On both the street, there are local peaks of signals where the open areas allow stronger signals to reach the street. Therefore, we can infer that the path loss is highly dependent on the geometries and distributions of buildings.

The means and standard deviations of errors between measurements and simulated predictions [17] on the two streets are also presented in Table 1. The ray tube method presented in [17] is similar to the proposed method in this paper. Both of them are applied to the quasi 3-D environments. According to the errors shown in Table 1, it could be observed that the RT method proposed here yielded better prediction accuracy compared to the ray tube method. On Slater Street, our simulated predictions are slightly larger than the measurements. Whereas, on Queen Street, our predicted results are less than the measurements. There are two main reasons for the case presented above. On the one hand, we have no detailed information of the build-

Table 1. Means and standard deviations of errors between predictions and measurements on the two streets.

Street	Proposed method		Ray tube method [17]	
	Mean	Standard Deviation	Mean	Standard Deviation
Slater St.	5.67 dB	5.17 dB	6.13 dB	6.14 dB
Queen St.	−5.76 dB	10.03 dB	−4.86 dB	10.50 dB

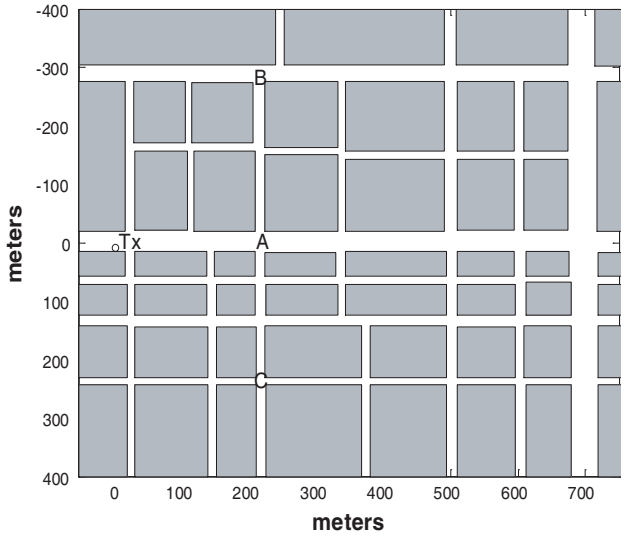

Figure 9. Plan view of a Tokyo street grid.

ings and streets in this area and the effects of other scatters such as trees and vehicles are not taken into account in our calculations, either. On the other hand, the rooftop diffracted signals give large portion of total received signals when there are many obstacles between Tx and Rx, but the rooftop diffractions are ignored in the proposed method.

Figure 9 shows another scene in Tokyo where measurements have been done at 1.48 GHz by Iwama and Mizuno [30], and was quoted by S. Y. Tan and H. S. Tan [8]. The Tx is positioned 5.3 m above the road surface and is close to the street side. A vertically polarized receiving antenna Rx is placed 3 m above the road surface, and its position is moved along the measuring street. Based on the geometry of Fig. 9, the signal path loss is computed along two measuring routes in Tokyo for comparison with the published measurements [30], with

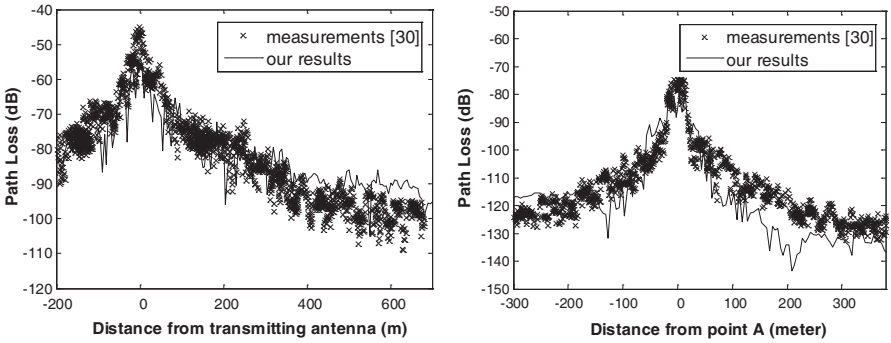

(a) (b)

Figure 10. Comparison of prediction versus measured path loss. (a) Along the LOS street. (b) Along the side street BAC near Shinbashi station in Tokyo.

Table 2. The computation time by our proposed method for Fig. 7 and Fig. 9.

Street	Slater Street in Fig. 7	Queen Street in Fig. 7	LOS street in Fig. 9	OOS street BAC in Fig. 9
Time	109 s	98 s	2 s	2 s

the values of $\varepsilon_r = 15$ and $\sigma = 7\,\mathrm{S/m}$ following the existing literature [8]. Fig. 10(a) and 10(b) show the simulation results for LOS street and OOS perpendicular street, respectively. In Fig. 10(b), it was obvious that near the junction, there was a significant increase of the received signal strength due to the LOS and the first-order reflected fields. As soon as the receiver moved away from the junction in OOS conditions, the second-order field prevailed, and the path-loss factor dropped abruptly. As for two scenarios mentioned above, the good agreement between measured and computed path-loss data indicated that the proposed quasi 3-D propagation method gives good results in such high-rise urban environments.

The computation times required to complete the prediction of each street in the two scenarios are also presented in Table 2 above. The simulations were carried out under a Windows operating system with Intel (R) Core (TM) i5 2.8 GHz processor and main memory of 4.0 GB. According to Table 2, the computation times for the two streets in the first scenario are obviously longer than the computation times in the second scenario due to comprise more faces and edges in the first

scene. And, the proposed method can quickly predict coverage in urban microcellular environments for above two mentioned scenarios.

5. CONCLUSION

In this paper, a novel quasi 3-D RT algorithm, based on creating a new virtual source tree in which the relationship between neighbor nodes is left-son-and-right-brother one can be applied to any complex propagation environment with composed of arbitrary-shaped buildings, streets and open areas. The proposed method is fundamentally a point-to-point tracing method, so reception tests are not required and it guarantees high accuracy. It was proven to have satisfactory prediction accuracy for 910 MHz and 1.48 GHz radio wave propagation in urban microcellular networks. In the process of executing RT procedure, a compromise between execution time and calculation accuracy is achieved by the creation of the new storage structure, definition of the type weight of the ray, limitation of limit number, acceleration of handling diffraction sources, and operation of generating the virtual source tree and finding propagation paths at one time. The proposed method, which has the better prediction accuracy than the ray tube method, is not optimized yet with respect to CPU times, but has a lot of potential to be made much faster. Future investigations will focus on the pre-process of input database (wall surfaces, wall edges, etc.,) and acceleration techniques by reducing the number of intersection tests in order to reduce the calculation time of the proposed method, without affecting the accuracy of the prediction. In this paper, the proposed RT algorithm can handle only buildings with vertical walls. However, many modern buildings are not constructed in that way. So, in our future work, these buildings are not constructed with vertical walls will also be taken into account.

ACKNOWLEDGMENT

The authors would like to thank Huawei Technologies CO., Ltd. for the financial support of this work (Contract No. YJCB2009028WL).

REFERENCES

1. Fuschini, F., H. El-Sallabi, V. Degli-Esposti, L. Vuokko, D. Guiducci, and P. Vainikainen, "Analysis of multipath propagation in urban environment through multidimensional measurements and advanced ray tracing simulation," *IEEE Trans. Antennas and Propag.*, Vol. 56, No. 3, 848–857, 2008.

2. Papkelis, E. G., I. Psarros, I. C. Ouranos, C. G. Moschovitis, K. T. Karakatselos, E. Vagenas, H. T. Anastassiu, and P. V. Frangos, "A radio-coverage prediction model in wireless communication systems based on physical optics and the physical theory of diffraction," *IEEE Antennas and Propagation Magazine*, Vol. 49, No. 2, 156–165, 2007.
3. Hata, M., "Empirical formula for propagation loss in land mobile radio services," *IEEE Trans. Veh. Tech.*, Vol. 29, No. 3, 317–325, 1980.
4. Ikegami, F., S. Yoshida, T. Takeuchi, and M. Umehira, "Propagation factors controlling mean field strength on urban streets," *IEEE Trans. Antennas and Propag.*, Vol. 32, No. 8, 822–829, 1984.
5. Phaiboon, S. and P. Phokharatkul, "Path loss prediction for low-rise buildings with image classification on 2-D aerial photographs," *Progress In Electromagnetics Research*, Vol. 95, 135–152, 2009.
6. Lee, H.-S., "A photon modeling method for the characterization of indoor optical wireless communication," *Progress In Electromagnetics Research*, Vol. 92, 121–136, 2009.
7. Lee, D. J. Y. and W. C. Y. Lee, "Propagation prediction in and through buildings," *IEEE Trans. Veh. Tech.*, Vol. 49, No. 5, 1529–1533, 2000.
8. Tan, S. Y. and H. S. Tan, "A microcellular communications propagation model based on the uniform theory of diffraction and multiple image theory," *IEEE Trans. Antennas and Propag.*, Vol. 44, No. 10, 1317–1326, 1996.
9. Kanatas, A. G., I. D. Kountouris, G. B. Kostaras, and P. Constantinou, "A UTD propagation model in urban microcellular environments," *IEEE Trans. Veh. Tech.*, Vol. 46, No. 1, 185–193, 1997.
10. Dimitriou, A. G. and G. D. Sergiadis, "Architectural features and urban propagation," *IEEE Trans. Antennas and Propag.*, Vol. 54, No. 3, 774–784, 2006.
11. Franceschetti, M., J. Bruck, and L. J. Schulman, "A random walk model of wave propagation," *IEEE Trans. Antennas and Propag.*, Vol. 52, No. 5, 1304–1317, 2004.
12. Blas Prieto, J., R. M. Lorenzo Toledo, P. Fernandez Reguero, E. J. Abril, A. Bahillo Martinez, S. Mazuelas Franco, and D. Bullido, "A new metric to analyze propagation models," *Progress In Electromagnetics Research*, Vol. 91, 101–121, 2009.
13. Kim, H. and H. Lee, "Accelerated three dimensional ray tracing

techniques using ray frustums for wireless propagation models," *Progress In Electromagnetics Research*, Vol. 96, 21–36, 2009.

14. Schuster, J. W. and R. J. Luebbers, "Comparison of GTD and FDTD predictions for UHF radio wave propagation in a simple outdoor urban environment," *IEEE Antennas and Propag. Society International Symposium*, Vol. 3, 2022–2025, 1997.
15. Kouyoumjian, R. G. and P. H. Pathak, "A uniform theory of diffraction for an edge in a perfectly conducting surface," *Proc. IEEE*, Vol. 62, No. 4, 1448–1462, 1974.
16. Gennarelli, G. and G. Riccio, "A uapo-based model for propagation prediction in microcellular environments," *Progress In Electromagnetics Research B*, Vol. 17, 101–116, 2009.
17. Son, H.-W and N.-H. Myung, "A deterministic ray tube method for microcellular wave propagation prediction model," *IEEE Trans. Antennas and Propag.*, Vol. 47, No. 8, 1344–1350, 1999.
18. Tayebi, A., J. Gomez, F. S. de Adana, and O. Gutierrez, "The application of ray-tracing to mobile localization using the direction of arrival and received signal strength in multipath indoor environments," *Progress In Electromagnetics Research*, Vol. 91, 1–15, 2009.
19. Song, H. B., H.-G. Wang, K. Hong, and L. Wang, "A novel source localization scheme based on unitary esprit and city electronic maps in urban environments," *Progress In Electromagnetics Research*, Vol. 94, 243–262, 2009.
20. Aguado Agelet, F., A. Formella, J. M. Hernando-Rabanos, F. I. de Vicente, and F. P. Fontan, "Efficient ray-tracing acceleration techniques for radio propagation modeling," *IEEE Trans. Veh. Tech.*, Vol. 49. No. 6, 2089–2104, 2000.
21. Degli-Esposti, V., F. Fuschini, E. Vitucci, and G. Falciasecca, "Speed-Up techniques for ray tracing field prediction models," *IEEE Trans. Antennas and Propag.*, Vol. 57, No. 5, 1469–1480, 2009.
22. Gomez, J., A. Tayebi, F. S. de Adana, and O. Gutierrez, "Localization approach based on ray-tracing including the effect of human shadowing," *Progress In Electromagnetics Research Letters*, Vol. 15, 1–11, 2010.
23. Mouysset, V., P. A. Mazet, and P. Borderies, "Efficient treatment of 3d time-domain electromagnetic scattering scenes by disjointing sub-domains and with consistent approximations," *Progress In Electromagnetics Research*, Vol. 71, 41–57, 2007.
24. Schettino, D. N., F. J. S. Moreira, and C. G. Rego, "Efficient

ray tracing for radio channel characterization of urban scenarios," *IEEE Transactions on Magnetics*, Vol. 43, No.4, 1305–1308, 2007.

25. Kim, B.-C., K. K. Park, and H.-T. Kim, "Efficient RCS prediction method using angular division algorithm," *Journal of Electromagnetic Waves and Applications*, Vol. 23, No. 1, 65–74, 2009.
26. Iskander, M. F. and Z. Yun, "Propagation prediction models for wireless communication systems," *IEEE Trans. Microwave Theory Tech.*, Vol. 50, No. 3, 662–673, 2002.
27. El-Sallabi, H. M. and P. Vainikainen, "Improvements to diffraction coefficient for non-perfectly conducting wedges," *IEEE Trans. Antennas and Propag.*, Vol. 53, No. 9, 3105–3109, 2005.
28. Whitteker, J. H., "Measurements of path loss at 910 MHz for proposed microcell urban mobile systems," *IEEE Trans. Veh. Tech.*, Vol. 37, No. 3, 125–129, 1988.
29. Tan, S. Y. and H. S. Tan, "Propagation model microcellular communications applied to path loss measurements in Ottawa city streets," *IEEE Trans. Veh. Tech.*, Vol. 44, No. 2, 313–317, 1995.
30. Iwama, T. and M. Mizuno, "Prediction propagation characteristics for microcellular laud mobile radio," *Proc. Int. Symp. Antennas Propagat.*, 421–424, Sapporo, Japan, 1992.